# Reconstruction of Magnetic Resonance Images Using One-Dimensional Techniques

K. P. Vassiliadis, *Student Member, IEEE*, P. A. Angelidis, *Student Member, IEEE*, and G. D. Sergiadis, *Member, IEEE*

***Abstract*— Whenever DFT (discrete Fourier transform) processing of a multidimensional discrete signal is required, one can apply either a multidimensional FFT (fast Fourier transform) algorithm, or a single-dimension FFT algorithm, both using the same number of points. That is, the dimensions of a "multidimensional" signal, and of its spectrum, are a matter of choice. Every multidimensional sequence is completely equivalent to a one-dimensional function in both "time" and "frequency" domains. This statement applied to MRI (magnetic resonance imaging) explains why one can reconstruct the slice by using either one-dimensional or two-dimensional methods, as it is already done in echo planar methods. In the commonly used spin warp methods, the image can be also reconstructed by either one- or two-dimensional processing. However, some artifacts in the images reconstructed from the original "zig-zag" echo planar trajectory, are shown to be due to the wrong dimensionality of the FFT applied.**

## I. Introduction

IN MANY experiments one has to deal with multidimensional digital signals. For signal processing reasons, the $n$-D ($n$-dimensional) FFT (fast Fourier transform), where $n$ is the signal's dimension, is often computed. Also, in many applications (as in magnetic resonance imaging, computerized tomography, etc.) one acquires the signal directly in the FT (Fourier transform) domain of the desired function (image) and thus the application of the $n$-D FFT is required. It may however be shown that as far as DFT (discrete Fourier transform) processing is concerned, one may replace the $n$-dimensional FFT by a 1-D (one-dimensional) FFT [1]. Therefore, from the DFT point of view, all discrete signals are essentially one-dimensional signals. The condition that must hold (except that the signal must be in a discrete form) is that the corresponding 1-D signal must "spread" in a periodical manner onto the $n$-D domain of the actual signal. This reduction of the signal's dimensions may result in a considerable simplification of the signal processing software.

In magnetic resonance imaging there already exist "working" examples of this reduction of the signal's dimensions. These are the echo planar and related methods [2], [3], where it is possible to reconstruct the 2-D image by the application of a 1-D FFT. In the approaches proposed in [4]–[10], the nonuniform sampling in the vertical direction of the original "zig-zag" echo planar trajectory is considered to be responsible for some reconstruction artifacts and phase error problems. These are due to the fact that the reconstruction is done by applying 2-D FFT methods along the "zig-zag" trajectory. In order to apply a 2-D FFT, one must sample in a rectangular pattern. Our analysis will clearly show that one has to apply a 1-D FFT algorithm to the "zig-zag" trajectory in order to obtain an artifact-free reconstructed image. We are going to give a new interpretation of this fact from the point of view of digital signal processing, and also generalize it to other magnetic resonance imaging methods, such as the standard spin warp method.

Echo planar images obtained by both the "zig-zag" and the blipped echo planar [11], [12] versions bear also other imaging artifacts, which are not due to the application of the 2-D FFT but they are due to inherent limitations of these methods. These limitations stem from the difficulties to implement the fast switching gradients [13]–[15], from the static field inhomogeneity, and from the T2 signal decay [9].

In the first part of this paper we describe the equivalence between the two-dimensional and one-dimensional discrete functions. In the second part we generalize the above equivalence and in the last part we adjust this property to magnetic resonance imaging reconstruction methods.

## II. The Conversion of a Two–Dimensional Function to a One–Dimensional Function

Let us suppose that we have a 2-D discrete function with $M \times N$ points. These samples can be arranged in the form of an $M \times N$ array $x(m, n)$. This 2-D sequence can be mapped to a 1-D sequence by the relation

$$y(p) = y(Nm + n) = x(m, n) \tag{1}$$

where $0 \leq m < M$ and $0 \leq n < N$. This mapping is essentially a transformation, from one set of 2-D data arranged in a 2-D array according to a double index, into another set of 1-D data arranged linearly according to a single index. The vector $y(p)$ is formed by stacking the columns of $x(m, n)$. The first $N$ elements of $y(p)$ are the elements of the first column of $x(m, n)$, the next $N$ are the elements of the second column, and so forth for all the $M$ columns of $x(m, n)$. Taking the 1-D

Manuscript received September 15, 1992; revised February 20, 1993. The associate editor responsible for coordinating the review of this paper and recommending its publication was Dr. E. M. Haacke.

The authors are with the Department of Telecommunications, School of Electrical Engineering, Aristotelian University of Thessaloniki, 54006 Thessaloniki, Greece.

IEEE Log Number 9213414.

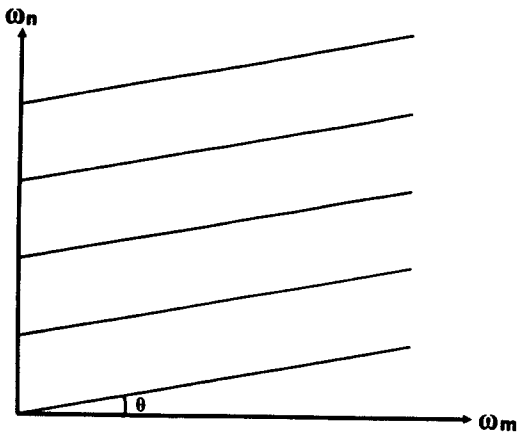


Fig. 1. The 1-D FT of $y(p)$ results in $N$ parallel line segments in the 2-D plane of $X(\omega_m, \omega_n)$. The angle $\theta$ is given by $\tan\theta = 1/N$.

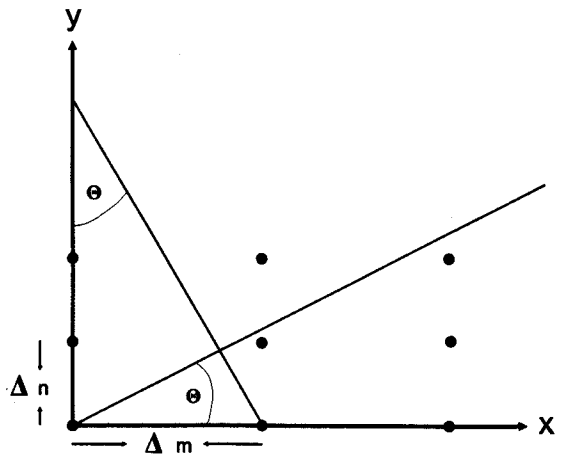


Fig. 2. The evaluation of the angle for which there is no overlap in the projection of a 2-D discrete function. Between the projection of two successive $m$, there must be enough space so that the $N$ pixels corresponding to each $m$ can be projected without overlapping. Therefore, $\Delta m \cos\theta = N\Delta n \sin\theta$, and thus $\theta = \tan(1/N)$ for $\Delta m = \Delta n$. In the figure $M = N = 3$.

FT of the sequence $y(p)$ we have

$$\begin{aligned} Y(\omega) &= \sum_{p=0}^{MN-1} y(p)\exp(-jp\omega) \\ &= \sum_{m=0}^{M-1}\sum_{n=0}^{N-1} y(Nm+n)\exp(-jNm\omega - jn\omega) \\ &= \sum_{m=0}^{M-1}\sum_{n=0}^{N-1} x(m,n)\exp(-jNm\omega - jn\omega). \end{aligned} \quad (2)$$

The 2-D FT (two-dimensional Fourier Transform) of the function $x(m,n)$ is

$$X(\omega_m, \omega_n) = \sum_{m=0}^{M-1}\sum_{n=0}^{N-1} x(m,n)\exp(-jm\omega_m - jn\omega_n). \quad (3)$$

The function $X(\omega_m, \omega_n)$ is periodic in both dimensions with a period of $2\pi$. Comparing (2) and (3), it is obvious that the 1-D FT of $y(p)$ equals the 2-D FT of $x(m,n)$ along the line $\omega_m = N\omega_n$ in the $X(\omega_m, \omega_n)$ plane. This line is at an angle $\theta = \tan^{-1}(1/N)$ to the $\omega_m$ axis, and due to the periodicity of $X(\omega_m, \omega_n)$, it becomes a set of $N$ parallel line segments, as is shown in Fig. 1. Since $x(m,n)$ can be recovered from $y(p)$, there must be a corresponding relation between $X(\omega_m, \omega_n)$ and $Y(\omega)$. In fact the function $Y(\omega)$ is a form of sampling of the function $X(\omega_m, \omega_n)$ along the $\omega_n$ direction [1].

It is interesting to note that the specific angle $\theta = \tan^{-1}(1/N)$ is the direction from which the $M \times N$ discrete function can be invertably projected [16]. That is, in this specific projection there is a one-to-one correspondence between the 2-D function and its 1-D projection. In this projection there exists enough free space between two successive $m$, so that the $N$ points of the corresponding column can be projected without overlapping. This means that, as shown in Fig. 2, $\Delta m \cos\theta = N\Delta n \sin\theta$ and for $\Delta n = \Delta m, \theta = \tan^{-1}(1/N)$. The function $y(p)$ is the projection of the function $x(m,n)$ from this angle. It is known [17] (central slice theorem) that the 1-D FT of a projection is equal to the slice of the 2-D FT of the original function, in the direction along which the projection has been taken. Therefore, $Y(\omega)$ is a slice of $X(\omega_m, \omega_n)$ in the $\theta = \arctan(1/N)$ direction, and due to the periodicity of $X(\omega_m, \omega_n)$, it is converted into $N$ equally spaced parallel line segments. The angle $\theta = \tan^{-1}(1/N)$ is usually called the "single projection angle," since the discrete object can be uniquely reconstructed from the single projection from this angle.

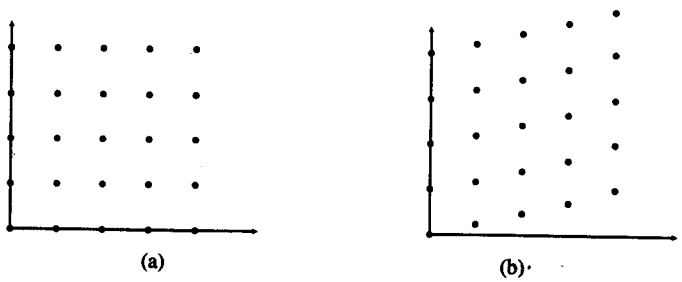


Fig. 3. (a) The points in the $X(\omega_m, \omega_n)$ plane which are evaluated by the 2-D DFT of the function $x(m,n)$ are shown. Notice that these points are arranged in a rectangular sampling pattern. (b) The points in the $X(\omega_m, \omega_n)$ domain which are evaluated by the 1-D DFT of the function $y(p)$ are shown. Notice the "rotated," or more accurately the "skewed," version of the sampling pattern as compared to Fig. 3(a). Naturally there are $M \times N$ points in both figures, placed in different locations but completely equivalent from the information point of view.

The 2-D DFT (two-dimensional discrete Fourier transform) of $x(m,n)$ is defined as

$$X(k_m, k_n) = \sum_{m=0}^{M-1}\sum_{n=0}^{N-1} x(m,n)\exp\left(-j\frac{2\pi}{M}mk_m - j\frac{2\pi}{N}nk_n\right). \quad (4)$$

The function $X(k_m, k_n)$ is a discrete periodic function with periods $M$ and $N$ in the $k_m$ and $k_n$ directions respectively, and is a set of $M \times N$, equally spaced independent samples of $X(\omega_m, \omega_n)$, arranged in a rectangular pattern, as it is shown in Fig. 3(a).

The 1-D DFT of $y(p)$ results in $M \times N$ equally spaced samples of the 1-D FT of $y(p)$ and therefore of the 2-D FT of $x(m,n)$. These samples are along the $N$ parallel line segments

of Fig. 1. There are $M$ equally spaced samples per line, as shown in Fig. 3(b). Although these samples are different from those of $X(k_m, k_n)$, they are completely equivalent to them, since they can be used to reconstruct $y(p)$ and therefore $x(m, n)$. These two sets of different samples have the same information content: their difference is due to a different choice of the 2-D sampling pattern [18]. In fact the sampling pattern used by $Y(k)$ is a "rotated," or more accurately a "skewed," version of that used by $X(k_m, k_n)$ which was the simple rectangular sampling pattern.

The mapping of (1) can be equivalently done using the function

$$z(p) = z(m + Mn) = x(m, n). \tag{5}$$

The vector $z(p)$ is formed by stacking the rows of $x(m, n)$, where the first $M$ elements are the first row of $x(m, n)$, etc. The 1-D FT of $z(p)$ is

$$\begin{aligned} Z(\omega) &= \sum_{p=0}^{MN-1} z(p)\exp(-jp\omega) \\ &= \sum_{m=0}^{M-1}\sum_{n=0}^{N-1} y(m + Mn)\exp(-jm\omega - jMn\omega) \\ &= \sum_{m=0}^{M-1}\sum_{n=0}^{N-1} x(m, n)\exp(-jm\omega - jMn\omega) \end{aligned} \tag{6}$$

and it corresponds to the line $\omega_m = (1/M)\omega_n$ in the $X(\omega_m, \omega_n)$ plane. Due to the periodicity of the $X(\omega_m, \omega_n)$ plane, this line becomes a set of $M$ parallel line segments.

Notice that the functions $y(p)$ and $z(p)$ are not the only functions one could choose for an invertable (in both spaces) mapping. For example we can use the functions $f(\kappa Nm + n) = x(m, n)$ and $g(m + \lambda Mn) = x(m, n)$ where $\kappa$ and $\lambda$ are any integers. Choosing one of these functions results into appending $\kappa N(\lambda M)$ zeros to each column (row) of $x(m, n)$ and changing the angle "$\theta$" in the Fourier domain [1]. From the point of view of the number of points required, it is clear that the functions $y(p)$ and $z(p)$ are optimal, since they have in both domains the same number of points as the original two-dimensional function had.

Therefore, from the DFT point of view, there is no point in speaking of a two-dimensional discrete sequence or of a discrete function's dimensions. Every two-dimensional discrete function is in both "time" and "frequency" domains completely equivalent to a 1-D function, with the same number of points. The two-dimensional discrete function can thus be recovered from the corresponding 1-D function. These results can be obviously generalized to more than two dimensions.

## III. The Optimal Trajectories for the Dimensional Reduction

There are many sampling patterns one can choose for the acquisition of a 2-D signal [18]. This can be done either by changing the spatial locations of the sensors (as in the case of geophysical signals) or by changing the experimental conditions during the acquisition period (as in the magnetic resonance imaging case). We show that the 1-D signal derived from "column" (1) or "row-row" (5) mappings, leads directly to the possibility of applying 1-D FT processing. Due to the duality properties of the FT, one can choose the trajectory shown in Fig. 1 and obtain, through 1-D FT processing, the samples in the other domain arranged in a "column by column" pattern. Generally one can choose any of the sampling patterns shown in Fig. 4, acquire the signal as a 1-D signal, and using a 1-D FT obtain the information in the corresponding FT domain. The arrows in the figure denote the sampling direction, both in "time" and "frequency" domains.

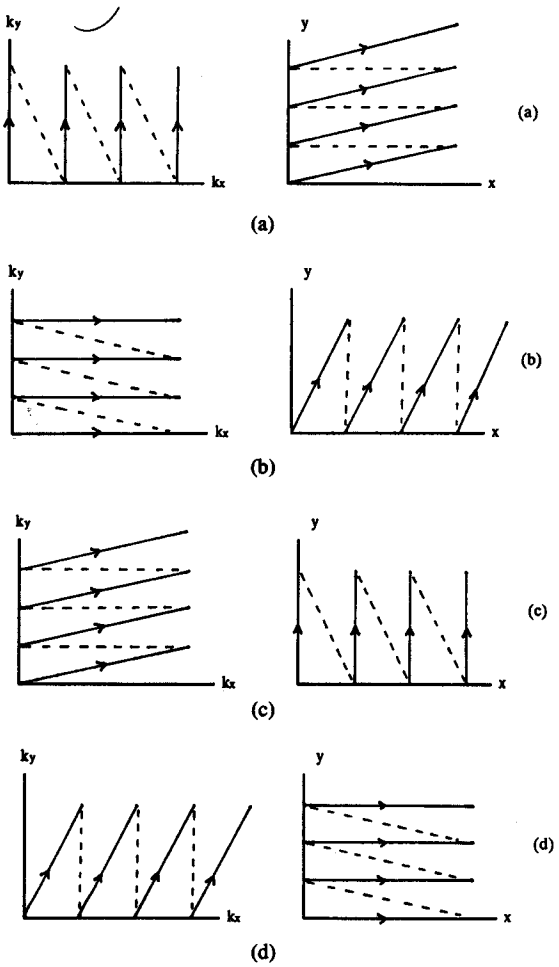


Fig. 4. The four optimal instances of recording the signal as a 1-D signal (left column) and the corresponding points in the 2-D FT domain (right column) that are calculated by applying the 1-D DFT to these particular signals. The arrows denote the sampling direction while the dashed lines denote the "jump" to the next point desired. It must be clear that these lines correspond to sets of samples and that they are not continuous lines.

Notice that for the application of a usual 2-D FFT, one must have the samples in a rectangular pattern, and the 2-D FFT also results in a rectangular pattern in the other domain. Although we can apply either a 1-D or a 2-D FFT in the rectangular pattern, and obtain a different set of samples every time, this is not the case for any of the "skewed" sampling patterns. That is, in the "skewed" pattern one has to apply a 1-D FFT. The alternate 1-D FFT (instead of 2-D) when applied to the rectangular pattern, results in a "skewed" version of the final samples in the FT domain. The four trajectories of Fig. 4 are the best that may be chosen, from the point of view of the number of points needed for 1-D processing of a 2-D signal.

## IV. Applications to Magnetic Resonance Imaging Methods

In MRI (magnetic resonance imaging) the signal is a slice in the 2-D Fourier plane of the distribution, or (central slice theorem) the 1-D FT of the projection of the distribution. By appropriately sampling the 2-D signal domain, that is, the 2-D FT domain of the image which is named K-space [19], [20], the image can be reconstructed using inverse FT methods.

In echo-planar methods, one acquires a single FID, along a k-space direction similar to that in Fig. 4(c) (as it will be shown), and the reconstruction must be done using a 1-D FFT algorithm, which is somewhat unexpected. However, we are going to show that it is nothing more than a mapping similar to that in (1). Echo planar methods are a "working" example of signal dimensionality reduction.

In the first version of echo planar methods [2] the proposed trajectory is the "zig-zag" trajectory of Fig. 5. The desired trajectory is obtained by using a constant gradient $Gy$ and an alternating gradient $Gx$. For a $M \times N$ image the relation between the intensities of the gradients is $G_x = NG_y$. Therefore the angle $\theta$ is given by $\arctan(1/N)$, because, in the first period, $kx(t) = G_x t = NG_y t$ and $K_y(t) = G_y t$. This is the same angle $\theta$, which results from the application of (1). However the trajectory of Fig. 5 is a little bit different from that of Fig. 1 (and of Fig. 4(c)). In Fig. 1 we show the first period of the periodical FT domain, and therefore the second half-period, corresponds to the negative frequencies. If we assume the usual convention in the FFT literature, that is if we fold the spectrum, we obtain the trajectory of Fig. 6. Notice that centering the signal results to a linear phase shift in the other domain and does not affect the amplitude of FFT after the quadrature demodulation. The difference between Figs. 5 and 6 is in every other line segment. More specifically, the even numbered (and of course the odd ones, too) lines in Fig. 6 are in the $\theta = \arctan(1/N)$ direction, whereas in Fig. 5 the even lines are in the $(\pi - \theta)$ direction. Notice, however, that in the case of discrete objects, the projection from the $\theta$ angle is the same as the projection from the $(\pi - \theta)$ angle. This is the case of echo planar methods, since in these methods the imposed periodicity in the time domain may be considered as an approximation of a discretization of the object being reconstructed [3]. In order to make the two trajectories absolutely identical, the points of every other line in Fig. 5 must be taken in reverse order. However this operation is commonly performed before applying the FFT algorithm to the "zig-zag" data. Therefore we conclude that the "zig-zag" trajectory of Fig. 5 is in fact completely equivalent to that of Fig. 1 and of Fig. 4(c), and therefore the echo planar method is an application of the mapping of a 2-D function to a 1-D function, according to (1).

Since the first version of echo planar imaging, there have been many methods based on the same idea of periodicity in the time (signal) domain. Every method uses a different trajectory in the k-space domain. Apparently, the "single projection angle" $\theta = \arctan(1/N)$ does not appear in these trajectories. For instance, in the blipped echo planar single pulse technique (BEPI) [11], [12], the trajectory is similar to that of the classical spin warp method [19], as it is shown in Fig. 7. In fact the only difference is that in blipped echo planar, the scanning trajectory direction alternates between odd and even lines, whereas in spin warp the scanning direction does not change. Consequently, a mere time reversal of half the data acquired will be adequate for the two scanning trajectories to become totally identical.

The observation of the similarity between these two scanning trajectories naturally leads to the following conclusion: If one can acquire the signal of the blipped echo planar as a 1-D signal, the same must be also true for the spin warp signal, since the two trajectories are in fact identical.

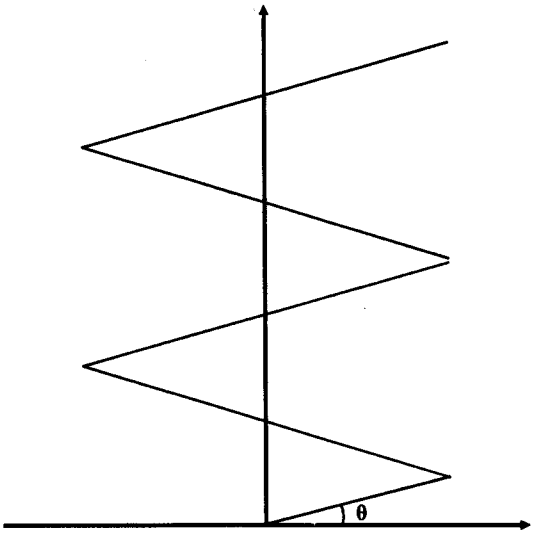


Fig. 5. The "zig-zag" trajectory of the original echo planar method. Notice that the angle, as determined from the gradients used, is the same as the "single projection angle," which results from the application of (1).

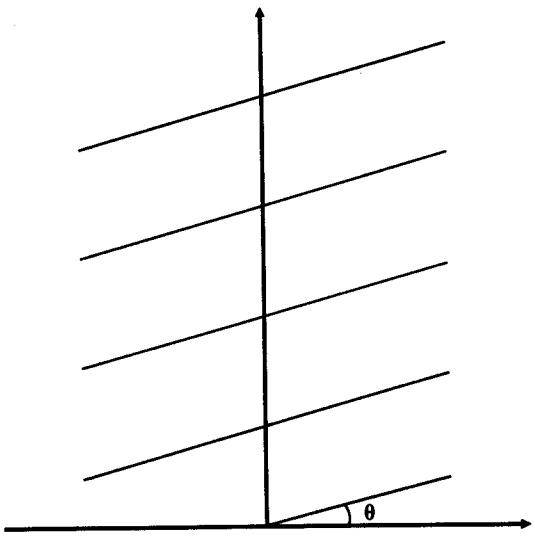


Fig. 6. The trajectory of Fig. 1 is unfolded (the negative half-period is after the positive one). By folding it, one obtains the trajectory of the above figure. Compare it with the one of Fig. 5.

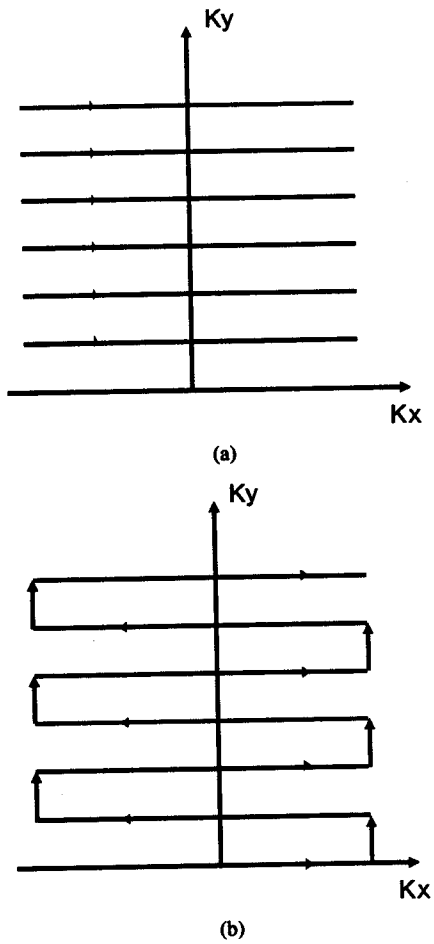


Fig. 7. The trajectories in the 2-D K-space of the (a) spin warp and (b) blipped echo planar single pulse technique. Notice the similarity between these two versions of k-space scanning trajectories. It is more than obvious that if one method is able to reconstruct the image by 1-D FT processing, the same must be also true of the other.

The first, original version of the echo planar method reconstructs the image as a 1-D function, column by column, and samples the k-space signal along the directions $\theta = \arctan(1/N)$ (Fig. 4(c)). Blipped echo planar samples the k-space signal line by line, along parallel lines in the direction $\theta = 0$ (as spin warp does) and reconstructs the image by a 1-D FFT along parallel lines in the direction $\theta = \arctan(M)$ (Fig. 4b). If a 2-D FFT algorithm is used, then the pattern in the image domain will also be rectangular. The above analysis constitutes a formal explanation of the observations reported in [12] concerning the number of dimensions of the FFT.

It must be noted that one can also acquire the spin warp signal as a 1-D signal and reconstruct (using a 1-D FFT) $M \times N$ equally spaced samples in a form similar to that of Fig. 4(b). Therefore it is a matter of choice whether one reconstructs the image acquired by the spin warp method by 1-D or by 2-D FFT algorithms, as it is already done in the blipped echo planar method. The only difference between the two algorithms is the "skewed" sampling pattern in the domain of the reconstructed image. The relations among the signals in the original "zig-zag" echo planar method, in the blipped echo planar method, and in the spin warp method are shown in Fig. 8.

The above analysis can be obviously generalized by applying 1-D processing to 3-D MRI methods.

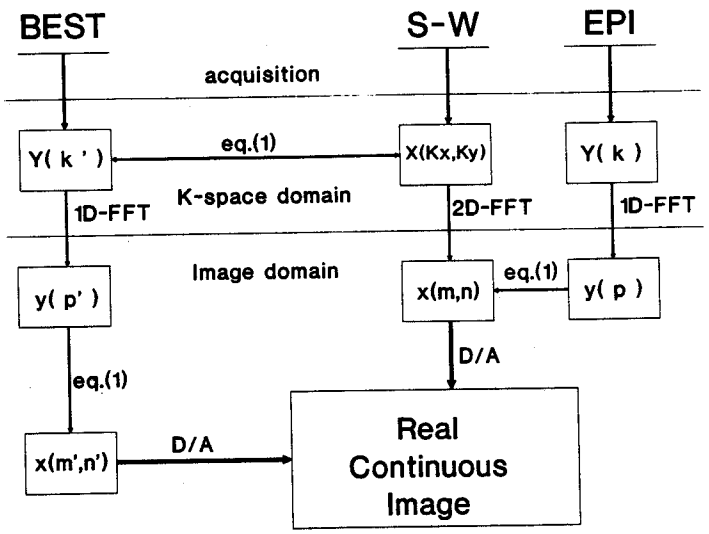


Fig. 8. The relations among the acquired signal and the reconstructed image in the original echo planar (EPI), the blipped echo planar (BEPI), and the spin warp (SW) methods. Notice that although the samples reconstructed are different, they are equivalent since the same continuous image is obtained after a D/A conversion.

## V. Conclusion

In this paper we have used the fact that any $M \times N$ 2-D discrete function is completely equivalent, in both "time" and "frequency" domains, to a 1-D function. We proposed a general interpretation of echo planar methods from the point of view of digital signal processing. We generalized the above analysis and proposed four optimal (from the point of view of the number of points required) trajectories for 1-D MRI acquisition and processing. One is the well known "zig-zag" echo planar and one of the others is the standard spin warp method. It is clear that the application of 1-D or 2-D reconstruction methods is, in the standard spin warp method, a matter of choice. One has only to interpret correctly the geometric locations of the points of the reconstructed image. However, there exist no such equivalence when using the "zig-zag" trajectory of the original planar method. The above analysis shows that various artifacts present in the reconstructed image, are the result of the application of the 2-D FFT in the "zig-zag" trajectory. We have shown that a 1-D FFT must be applied in this specific trajectory, and we have generalized the concept of the 1-D processing of a 2-D signal to other MRI methods.

## References

[1] R. M. Mersereau and D. E. Dudgeon, "The representation of two-dimensional sequences as one-dimensional sequences," *IEEE Trans. ASSP*, vol. ASSP–22, no. 5, pp. 320–325, 1974.
[2] P. Mansfield, "Multi-planar image formation using NMR spin echoes," *J. Phys. C: Solid State Phys.*, vol. 10, pp. L55–L58, 1977.
[3] P. Mansfield and I. L. Pykett, "Biological and medical imaging by NMR," *J. Mag. Res.*, vol. 29, pp. 355–373, 1978.
[4] H. Yan and M. Braun, "Image reconstruction from Fourier domain data sampled along a zig-zag direction," *Magn. Reson. Med.*, vol. 18, pp. 405–410, 1991.
[5] H. Yan and J. Mao, "Noise reduction in MR echo planar image reconstruction," *IEEE Trans. Med. Imaging*, vol. 10, pp. 148–153, 1991.

[6] G. C. Kashmar and O. Nalcioglu, "An improved echo planar reconstruction method," *IEEE Trans. Nucl. Scien.*, vol. 35, no. 1, pp. 744–748, 1988.
[7] L. F. Feiner and P. R. Locher, "On NMR spin imaging by magnetic field modulation," *Appl. Phys.*, vol. 22, pp. 257–271, 1980.
[8] M. M. Tropper, *J. Magn. Reson.*, vol. 42, pp. 193–202, 1981.
[9] F. Farzaneh, S. J. Riederer, and N. J. Pelc, "Analysis of T2 limitations and off resonance effects on spatial resolution and artifacts in echo planar imaging," *Magn. Reson. Med.*, vol. 14, pp. 123–139, 1990.
[10] K. Sekihara and H. Kohno, "New reconstruction technique for echo-planar imaging to allow combined use of odd and even numbered echoes," *Magn. Res. Med.*, vol. 5, pp. 485–491, 1987.
[11] M. Doyle *et al., Lancet* 2, 682, 1986.
[12] R. J. Ordidge *et al.*, "Snapshot head imaging at 0.5T using the echo planar technique," *Magn. Reson. Med.*, vol. 8, pp. 110–115, 1988.
[13] G. Kashmar and O. Nalcioglu, "Cartesian echo planar hybrid scanning with two to eight echoes," *IEEE Trans. Med. Imag.*, vol. 10, pp. 1–10, 1991.
[14] H. Bruner *et al.*, "Image reconstruction for echo planar imaging with nonequidistant k-space sampling," *Magn. Reson. Med.*, vol. 23, pp. 311–323, 1992.
[15] A. Zakhor, R. Weisskoff, and R. Rzedzian, "Optimal sampling and reconstruction of MRI signals resulting from sinusoidal gradients," *IEEE Trans. Sig. Proces.*, vol. 39, no. 9, pp. 2056–2065, 1991.
[16] R. M. Mersereau and A.V. Oppenheim, "Digital reconstruction of multidimensional signals from their projections," *Proc. IEEE*, vol. 62, no. 10, pp. 1319–1338, 1974.
[17] R. A. Brooks and G. Di Chiro, "Principles of computer assisted tomography (CAT) in radiographic and radioisotopic imaging," *Phys. Med. Biol.*, vol. 21, no. 5, pp. 689–732, 1976.
[18] D.E. Dudgeon and R.M. Mersereau, *Multidimensional Digital Signal Processing*. Englewood Clifs, NJ: Prentice Hall, 1984.
[19] S. Ljunggren, "A simple graphical representation of Fourier-based imaging methods," *J. Magn. Res.*, vol. 54, pp. 338–343, 1983.
[20] D. B. Twieg, "The k-trajectory formulation of the NMR imaging process with applications in analysis and synthesis of imaging methods," *Med. Phys.*, vol. 10, no. 5, pp. 610–621, 1983.